

FEDSM-ICNMM2010-' 0)) (

MODELING OF BLOOD FLOW IN THE HUMAN BRAIN

**Md.Shahadat Hossain, Bhavin Dalal, Ian S Fischer and
Pushendra Singh**

Department of Mechanical and Industrial Engineering
New Jersey Institute of Technology
Newark, New Jersey 07102, U.S.A.

Nadine Aubry

Department of Mechanical Engineering
Carnegie Mellon University
Pittsburgh, PA 15213, U.S.A.

1. ABSTRACT

The non-Newtonian properties of blood, i.e., shear thinning and viscoelasticity, can have a significant influence on the distribution of Cerebral Blood Flow (CBF) in the human brain. The aim of this work is to quantify the role played by the non-Newtonian nature of blood. Under normal conditions, CBF is autoregulated to maintain baseline levels of flow and oxygen to the brain. However, in patients suffering from heart failure (HF), Stroke, or Arteriovenous malformation (AVM), the pressure in afferent vessels varies from the normal range within which the regulatory mechanisms can ensure a constant cerebral flow rate, leading to impaired cerebration in patients. It has been reported that the change in the flow rate is more significant in certain regions of the brain than others, and that this might be relevant to the pathophysiological symptoms exhibited in these patients. We have developed mathematical models of CBF under normal and the above disease conditions that use direct numerical simulations (DNS) for the individual capillaries along with the experimental data in a one-dimensional model to determine the flow rate and the methods for regulating CBF. The model also allows us to determine which regions of the brain would be affected relatively more severely under these conditions.

Keywords:

Arteriovenous malformation, Cerebral blood flow, Direct numerical simulation, Heart failure, Shear thinning, Simulation, Stroke, Viscoelasticity

2. INTRODUCTION

According to the American Heart Association and the National Institute of Health, about 5.7 million people in the United States are living with heart failure which results in about 300,000 deaths each year. The number of people with heart failure is growing, and each year an additional 670,000 people are diagnosed for the first time.

The brain is a vital organ in the human body, and stable perfusion is necessary to maintain its functionality. The human brain is especially sensitive to the circulatory changes that reduce oxygen and glucose delivery. Patients with heart failure are generally considered to have reduced CBF and suffer from neuropsychological problems such as cognitive impairment with lethargy, confusion, memory problems, and dizziness which may increase morbidity in patients with severe chronic heart failure (CHF). Cerebral circulation, which is a significant portion of the cardiac output, is regulated to maintain a relatively-constant value of the perfusion pressure in response to metabolic and physiological demands. Cerebral circulation depends on many parameters, one of which is the mean arterial pressure (MAP).

Stroke ranks third among the leading causes of death and is the leading cause of disability in older adults [1]. More than 700,000 new and recurrent strokes occur each year, resulting in over 163,000 deaths in the United States.

A stroke occurs when a blood vessel that brings oxygen and nutrients to the brain either bursts (hemorrhagic stroke) or is clogged by a blood clot or some other mass (ischemic stroke). Most of these strokes occur when a cerebral aneurysm or brain AVM ruptures. When a rupture or blockage occurs, parts of the brain do not get the blood and oxygen they need. Without oxygen, nerve cells in the affected area of the brain cannot work properly, and die within minutes—usually within 3 to 4 minutes. The ultimate effect of hemorrhagic strokes is either death or a major disability.

The flow characteristics of blood depend on the concentration of red blood cells (RBCs), the blood vessel diameter and the flow rate. At low shear rates ($< 100 \text{ s}^{-1}$), the RBCs cluster to form a rouleaux which disperses as the shear rate increases, reducing the viscosity of blood. The resulting shear-thinning behavior caused by rouleaux disaggregation in blood plasma is responsible for the non-Newtonian behavior of

blood. However, with further increase in shear rate, at least in the devices that have simple shear flows, the shear-thinning characteristics disappear [2-7].

The goal of our research work is to develop a comprehensive mathematical model for the human cerebral circulation for both normal and pathological conditions, which can be used to predict the blood flow rates in different regions of the brain for different pathological conditions, such as AVM, Heart Failure, and Stroke.

3. METHOD

3.1 Structure

The anatomical structure of the brain model is comprised of a network of blood vessels (Fig. 1). A group of identical vessels, referred to as a compartment in earlier studies [8-11], is used as an element in our model.

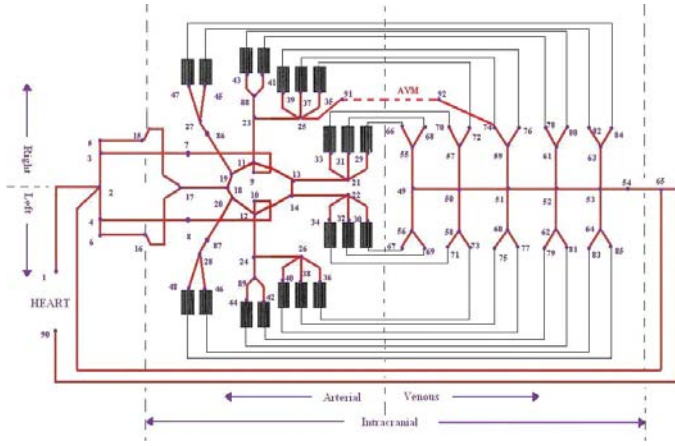


Figure 1: Schematic diagram of the model of the intracranial blood vessel network. A thicker line represents a compartment that contains several identical vessels in parallel. The numbers indicate the nodes. There are 20 microvessel groups (MVG) between the arteries and the veins, each of which consists of 5000 microvessels. A thinner line between a MVG and a vein does not represent a compartment, but a connection between the two compartments.

3.2 Mathematical and computational approach

The governing mass and momentum conservation equations for the motion of a shear-thinning Oldroyd-B liquid, which will be used to model blood, can be written as

$$\nabla \cdot \mathbf{u} = 0, (1)$$

$$\rho \left(\frac{\partial \mathbf{u}}{\partial t} + \mathbf{u} \cdot \nabla \mathbf{u} \right) = \rho \mathbf{g} - \nabla p + \nabla \cdot \left(\frac{c}{De} \mathbf{A} \right) + \nabla (2\mu \mathbf{D}).$$

These equations are subjected to velocity boundary conditions at the solid boundaries. The evolution of the configuration tensor \mathbf{A} , which gives the viscoelastic stress, is given by

$$\frac{\partial \mathbf{A}}{\partial t} + \mathbf{u} \cdot \nabla \mathbf{A} = \mathbf{A} \cdot \nabla \mathbf{u} + \nabla \mathbf{u}^T \cdot \mathbf{A} - \frac{1}{\lambda_r} (\mathbf{A} - \mathbf{I}).$$

Here, \mathbf{u} is the velocity, p is the pressure, $\boldsymbol{\sigma} = \frac{c\eta_s}{\lambda_r} \mathbf{A} + 2\eta_s \mathbf{D}$ is

the extra stress tensor, ρ_L is the density, \mathbf{D} is the symmetric part of the velocity gradient tensor, c is a measure of viscoelasticity in terms of its contribution to the zero shear viscosity, and λ_r is the relaxation time. The fluid viscosity $\eta = \eta_s + \eta_p$, where $\eta_p = c \eta_s$ is the viscoelastic contribution to viscosity and η_s is the purely viscous contribution to viscosity. The fluid-retardation time is equal to $\frac{\lambda_r}{1+c}$. This model has been used in several

previous studies to model the viscoelastic nature of blood.

Shear thinning is incorporated into the Oldroyd-B model by assuming that the total viscosity varies according to the Carreau–Yasuda model [12-16]:

$$\frac{\mu - \mu_\infty}{\mu_0 - \mu_\infty} = \left[1 + (\lambda_3 \dot{\gamma})^a \right]^{\frac{n-1}{a}}. (1)$$

Here $\dot{\gamma}$ is the strain rate defined in terms of the second invariant of the symmetric part of the velocity gradient tensor $\dot{\gamma} = \sqrt{2\mathbf{D} : \mathbf{D}}$, μ_0 is the zero shear viscosity, μ_∞ is the minimum value of viscosity which is achieved when the shear rate approaches infinity, n is a parameter between 0 and 1, and λ_3 is a parameter. The values of these parameters used in [10] for blood were: $\mu_0 = 0.022$ Pa.s, $\mu_\infty = 0.0022$ Pa.s, $\lambda_3 = 0.11$ s, $a = 0.644$, and $n = 0.392$.

The flow in the MVGs will be modeled as a porous medium flow and incorporated at the end of each of the efferent tubes. The flow resistance of the MVGs will be varied to model the autoregulation mechanism.

The above equations can be made dimensionless by assuming that the characteristic length, velocity, time, stress and angular velocity scales are D , U , D/U , $\eta U/H$ and U/D , respectively. It is easy to show that the governing dimensionless parameters in the above equations are: the

$$\text{Reynolds number } \text{Re} = \frac{\rho_L U D}{\eta}, \text{ the Deborah number } \text{De} = \frac{\lambda_r U}{D}, \text{ and the parameters in the Carreau–Yasuda model.}$$

Notice that the physical problem is governed by several dimensionless parameters and it is important that each of these parameters be matched to its corresponding value for the flow in the circle of Willis (CoW) (2)

The well-known approximation for single-vessel hemodynamics is the Hagen-Poiseuille equation which is used in our models to calculate the volumetric flow rate of blood through different compartments of the network of blood vessel at different pressure gradients [12].

$$Q = \frac{\pi D^4}{132\mu L} \Delta P \quad (2)$$

where Q is the volumetric blood flow rate through the vessel, ΔP is the pressure drop across the vessel, D is the inner diameter of the vessel, L is the length, and μ is the blood dynamic viscosity ($= 0.0035$ Pa.s for normal, heart-failure and stroke models).

The effect of elasticity on the vessel diameter is modeled using the approach described in Ornstein et al. [17]. If the internal pressure of the vessel is P , the relation between D and P is given by

$$D = D(0)(1 + mP), \quad (3)$$

where $D(0)$ is the vessel radius at $P = 0$, and m is the elastic coefficient of the vessel. This equation is used to simulate the flow in different compartments for which the elastic coefficients are different.

The entire intracranial cerebral tissue and its perfusing microvessels were divided into 20 identical segments or micro vessel groups (MVGs), each of which is perfused by three smaller conductance arteries. Using the Hagen-Poiseuille law, the wall shear stress of each of the vessels in the network was expressed in terms of the volumetric flow rate [18]

$$\tau = \frac{32\mu Q}{\pi D^3}. \quad (4)$$

It has been observed clinically that a conductance blood vessel dilates if there is additional blood flow through the vessel. Although the mechanisms of vessel dilation remain unclear, the shear stress on the vessel wall is considered to be one of the possible factors [19, 20].

The model described in figure 1 consists of 113 elements, and each element has a diameter and a length. In order to determine the effect of a small AVM on the flow rate, we added three more elements in the model for the AVM compartment. The meeting junction of two or more elements is called a node. Each node has a unique number that is given in Fig. 1. The model has 90 nodes, except for the model that includes an AVM in which case there are 92 nodes.

In our model, the heart is the pump which drives the flow through the vessels. The pressure is assumed to be 120/80 mm Hg for the normal case, 220/120 mm Hg for the stroke case and 80/30 mm Hg for the heart-failure case.

The model allows us to compute the circulation of blood in the brain, i.e., it gives the volumetric flow rate and the wall shear stress in the elements, and the pressure at the node under normal and disease conditions

4. RESULTS

In Fig. 2 we show the pressure distribution in the middle cerebral artery (MCA) of the brain for the non-Newtonian case under normal conditions. Here E denotes node 7; I denotes node 11; T denotes node 23; H is the halfway point between T

and the feeding artery (node 90); aM denotes the arterial side of the microvessels (node 37); vM denotes the venous side of the microvessels (node 74); Sv denotes the small vein (node 59); Mv denotes the medium vein (node 51); Lv denotes the large vein (node 53); and E, I, T, H are the vascular zones taken from Fogarty-Mack et al. [21].

In Fig. 3 we show the pressure distribution for the same region of the brain when a small AVM is included in the model. For the AVM model, the pressure at zone E, T, vM are about 88.1 mm Hg, 73.6 mm Hg, 28.9 mm Hg, respectively, whereas in the normal model it is about 95.1 mm Hg, 77.9 mm Hg, 10.4 mm Hg respectively. Due to the presence of the AVM, the pressure in some of the regions is higher than for the normal model, and in some of the regions it is lower.

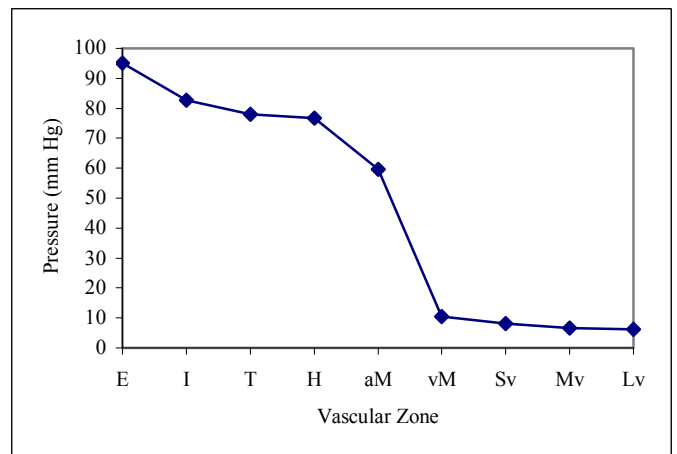


Figure 2: Pressure distributions of the middle cerebral artery (MCA) for the normal case in the various vascular zones of Figure 1.

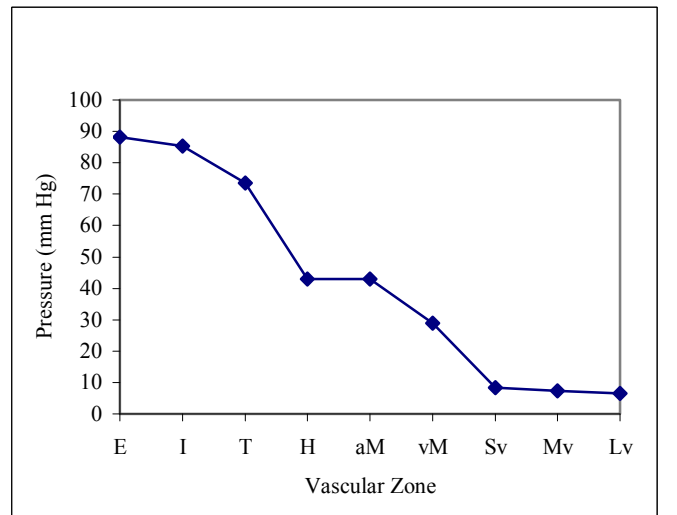


Figure 3: Pressure distributions of the middle cerebral artery (MCA) for the normal case with a small AVM in the various vascular zones of Figure 1, showing the effect of a small AVM.

The model also allows us to determine the shear stress in each of the vessels due to the blood flow under the normal condition and when an AVM is present. The shear stress values determined from this model are comparable with the published data by Lipowsky, 1995 [22]. In Fig. 4, we show the shear-stress distribution for the middle cerebral artery (MCA), its branches, and the draining veins. Here LA denotes large MCA arteries; SA denotes small arteries; Mic denotes the microvessels; SV denotes small veins; LV denotes large veins. The maximum shear stress is in the small arteries at about 29.5 dyne/cm², and the minimum shear stress in the large veins which is about 2.3 dyne/cm². Except for the large arteries, the calculated shear stresses are close to previously reported results.

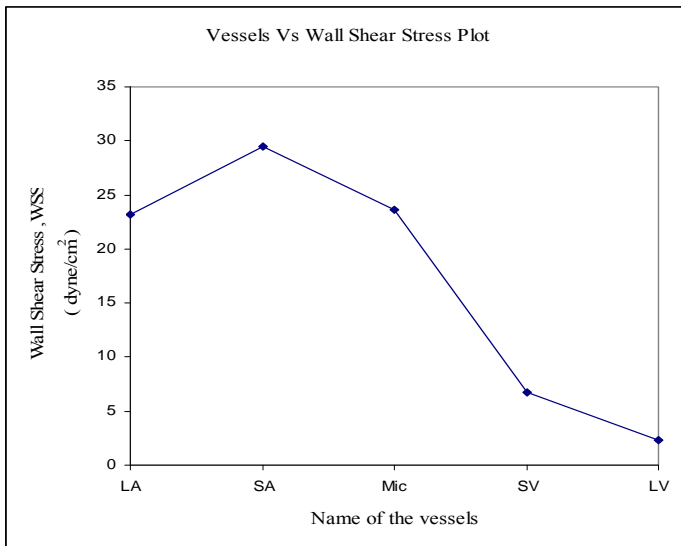


Figure 4: The shear stresses on the wall of the middle cerebral artery (MCA) and its branches, and in the draining veins in the normal model.

Figs. 5 and 6 show the change in the blood flow rate in the left and right MVG regions for the normal model, the dilated normal model, the normal model with a small AVM, the heart-failure model, and the stroke model. From these figures we note that the right and left MVG regions are getting an increased flow for the stroke model and decreased flow in the heart failure model, except for the model with added AVM in MCA2. For the latter case, MVG is not getting any flow and MCA1 and MCA3 are getting less flow than that for the HF model. Due to the presence of this particular AVM in the model, the right MCA1 is receiving about 48.6% less flow than for the normal model and on the other side, the left ACA3 is receiving about 15.6% more flow than for the normal model. In the model for the heart-failure case, the right and left ACA1 and ACA2 are very much affected and these MVGs are receiving about 144.5% less flow than for the normal model. On another end, the right and left MCA1 in the stroke model are receiving about 90.4% more flow than in the normal model.

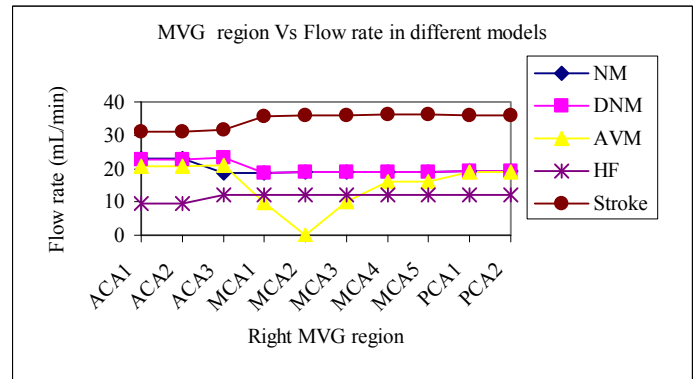


Figure 5: Cerebral blood flow distribution in the right MVG region for the normal and dilated models, the model with a small AVM, the Heart Failure model, and the Stroke model.

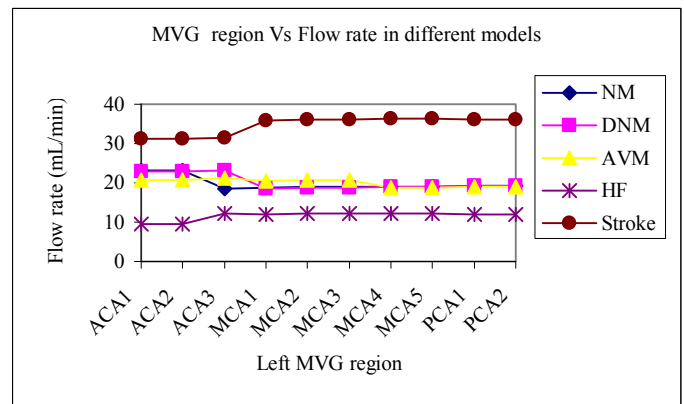


Figure 6: Cerebral blood flow distribution in the left MVG region for the normal model, the dilated model, the model with a small AVM, the Heart Failure model, and Stroke model.

5. CONCLUSIONS

Our one-dimensional model allowed us to compute the pressure and the shear-stress distribution for the network of blood vessels in the brain under different physiological conditions, as well as the change in the flow rate due to the vessel elasticity and the presence of an AVM. The Heart-Failure model reveals that in the MVG region, the decreases in the blood flow rate is maximal in the left and right ACA1 and ACA2, and that the decrease is about 59.1%. In the MCA, the blood flow decreases by 36.2% and by about 37.7% in the PCA. In the ACA region, it decreases by about 52.1%. The Stroke-patient model shows that in the MVG region, the maximum increases in the blood flow rate are in the left and right MCA1 where the increase is about 90.4%. In the MCA region, the blood flow increases by 89.7% and in the PCA by 88.1% region. In the ACA region, the increase is 44.7%.

6. REFERENCES

- [1] Broderick J., Brott T., Kothari R., Miller R., Khoury J., Pancioli A., Gebel J., Mills D., Minneci L., Shukla R., 1998, "The Greater Cincinnati/Northern Kentucky Stroke Study: Preliminary first-ever and total incidence rates of stroke among blacks," *Stroke*; Vol. 29, pp. 415–421.
- [2] Pop G.A.M., Hop W.J., van der Jagt M., Quak J., Dekkers D., Chang Z., Gijsen F.J., Dunncker D.J., Slager C.J., 2003, "Blood Electrical Impedance Closely Matches Whole Blood Viscosity as Parameter of Hemorheology and Inflammation," *Appl. Rheol.*; Vol. 13, pp. 305–312.
- [3] Kang I.S., 2002, "A Microscopic Study on the Rheological Properties of Human Blood in Low Concentration Limit," *Korea-Australia Rheology Journal*; Vol. 14, pp. 77–86.
- [4] Berger S., Jou L., 2000, "Flows in Stenotic Vessels," *Annual Review of Fluid Mechanics*; Vol. 32, pp. 347–382.
- [5] Boryczko K., Dzwinel W. et al., 2003, "Dynamical Clustering of Red Blood Cells in Capillary Vessels," *Journal of Molecular Modeling*; Vol. 9, pp. 16–33. [PubMed: 12638008]
- [6] Ku D.N., 1997, "Blood Flow in Arteries," *Annual Review of Fluid Mechanics*; Vol. 29, pp. 399–434.
- [7] Wootton D.M., Ku N.K., 1999, "Fluid Mechanics of Vascular Systems, Diseases, and Thrombosis," *Annual Review of Biomedical Engineering*; Vol. 1, pp. 299–329.
- [8] Hademenos GJ, Massoud TF & Vinuela F., 1996, "A biomathematical model of intracranial arteriovenous malformations based on electrical network analysis: theory and hemodynamics," *Neurosurgery*; Vol. 38, pp. 1005-1015.
- [9] Lo E.H., Fabrikant J.I., Levy R.P., Phillips M.H., Frankel K.A. & Alpen E.L., 1991, "An experimental compartmental flow model for assessing the hemodynamic response of intracranial arteriovenous malformations to stereotactic radiosurgery," *Neurosurgery*; Vol. 28, pp. 251-259.
- [10] Nagasawa S., Kawanishi M., Kondoh S., Kajimoto S., Yamaguchi K. & Ohta T., 1996, "Hemodynamic simulation study of cerebral arteriovenous malformations. Part II. Effects of impaired autoregulation and induced hypotension," *J. Cereb. Blood Flow Metab.*; Vol 16, pp. 162-169.
- [11] Gao E., Young W.L., Ornstein E., Pile-Spellman J. and Qiyuan M., 1997, "A Theoretical Model of Cerebral Hemodynamics: Application to the Study of Arteriovenous Malformations," *Journal of Cerebral Blood Flow & Metabolism*; Vol. 17, pp. 905-918.
- [12] Hademenos G.J., Massoud T.F. and Vinuela F., 1996, "A biomathematical model of intracranial arteriovenous malformations based on electrical network analysis: theory and hemodynamics," *Neurosurgery*; Vol. 38, pp. 1005-1015.
- [13] Bird, R.B., Armstrong, R.C., Hassager, O., 1987, *Dynamics of Polymer Liquids*, Vol. 1, 2nd edition. Wiley, New York.
- [14] Chien, S., Usami, S., Dellenback, R.J., Gregersen, M.I., 1970, "Shear dependent deformation of erythrocytes in rheology of human blood," *American Journal of Physiology*; Vol. 219, pp. 136–142.
- [15] Thurston, G.B., 1973, "Frequency and shear rate dependence of viscoelasticity of human blood," *Biorheology*; Vol. 10, pp. 375–381.
- [16] Thurston, G.B., 1979, "Rheological parameters for the viscosity, viscoelasticity and thixotropy of blood," *Biorheology*; Vol. 16, pp. 149–162.
- [17] Ornstein E., Blesser W.B., Young W.L. & Pile-Spellman, J., 1994, "A computer simulation of the hemodynamic effects of intracranial arteriovenous malformation occlusion," *Neurol Res.*; Vol. 16, pp. 345-352.
- [18] Hademenos, G.J. and Massoud T.F., 1996, "Risk of intracranial arteriovenous malformation rupture due to venous drainage impairment. A theoretical analysis," *Stroke*; Vol. 27, pp. 1072-1083.
- [19] Bevan J.A. and Laher, I., 1991, "Pressure and flow-dependent vascular tone [Review]," *FASEB J.*; Vol. 5, pp. 2267-2273.
- [20] LaBarbera M., 1995, "The design of fluid transport systems: a comparative perspective," (In) *Flow-Dependent Regulation of Vascular Function: Clinical Physiology Series*, American Physiological Society (Bevan JA, Kaley G, Rubanyi GM, eds.) New York, Oxford University Press, pp. 3-27.
- [21] Fogarty-Mack P., Pile-Spellman J., Hacin-Bey L., Osipov A., DeMeritt J., Jackson E.C. & Young W.L., 1996, "The effect of arteriovenous malformations on the distribution of intracerebral arterial pressures," *Am. J. Neuroradiol.*; Vol. 17, pp. 1443-1449.
- [22] Lipowsky H.H., 1995, "Shear stress in the circulation. (In) *Flow-Dependent Regulation of Vascular Function: Clinical Physiology Series*," American Physiological Society (Bevan JA, Kaley G, Rubanyi GM, eds.) New York, Oxford University Press, p. 32.